Open Access, Peer Reviewed, Research Journal

Print & Online available on https://jesbulletin.in
Research Article

Investigation of Theoretical Mass Attenuation Coefficients of water-soluble organic compound at Different Gamma Ray Energies, for the Radiation Shielding Applications

Sneha Dinkar Sanap[1,], S.R. Mitkari[1], Anil V. Raut[2], Pravina P. Pawar[3]*

[1]*Department of Physics, Shri. Siddheshwar Mahavidyalaya, Majalgaon, Dist. Beed, 431131 INDIA*
[2]*Department of Physics, Vivekanand Arts, Sardar DalipSingh Commerce and Science College, Aurangabad 431001 INDIA*
[3]*Department of Physics, Dr. Babasaheb Ambedkar Marathwada University, Aurangabad, 431001 INDIA*
Corresponding Author: snehasanap12@gmail.com

ARTICLE INFO

Received: 10/02/2024
Revised: 15/03/2024
Accepted: 01/04/2024

KEYWORDS

Mass Attenuation Coefficient; Gamma Ray; Radiation Shielding; Phy-X;

ABSTRACT

This research paper explores the mass attenuation coefficient (μ/ρ) of glucose (C6H12O6), a water-soluble inorganic compound, for its potential use in gamma-ray shielding applications. Theoretical calculations of the linear attenuation coefficient (μ) were performed using the Phy-X database following radioisotopes: 133Ba (356) keV, 22Na (511 and 1275) keV, 137Cs (662) keV, and 60Co (1173 and 1333) keV. The study found that the mass attenuation coefficient (μ/ρ) was highest at photon energies below 200 keV and decreased as photon energy increased. Key shielding parameters, including relaxation length (λ), half-value layer (HVL), tenth-value layer (TVL), effective atomic number (Zeff), and effective atomic weight (Aeff), were evaluated. The effective atomic number (Zeff) was specifically calculated to determine glucose's shielding efficiency. The research paper highlights that C6H12O6 exhibits notable gamma-ray shielding properties at low-energy radiation levels, suggesting its potential suitability for specific radiation shielding applications.

1 Introduction

In the context of space exploration, shielding spacecraft and instruments from cosmic gamma rays is vital for protecting astronauts and ensuring the functionality of sensitive equipment. Traditionally, dense materials such as lead and concrete have been the primary choices for gamma ray shielding due to their strong attenuation properties. However, concerns about the environmental and health risks associated with lead, along with the need for lighter, more versatile materials, have driven the search for alternative shielding solutions. Water-soluble organic compounds, such as glucose (C6H12O6), have emerged as promising candidates due to their lower density, cost-effectiveness, and adaptability. Advancements in radiation protection technology have significantly improved the evaluation and development of shielding materials. Modern techniques, such as using high-resolution detectors like NaI(Tl) in narrow-beam geometries, enable precise measurements of the mass attenuation coefficient (μ/ρ) for different substances. Computational tools such as Phy-X, an advanced online database for radiation shielding and interaction parameters, play a crucial role in these developments. The Phy-X database is a powerful and comprehensive platform specifically designed to calculate essential shielding and attenuation parameters for gamma rays and X-rays. It serves as a valuable resource for researchers, engineers, and scientists working in radiation protection and materials science. By leveraging advanced algorithms and theoretical models, Phy-X provides precise and reliable data that supports the design and evaluation of shielding materials across a variety of applications [1-6].

2 Phy-X Photon Shielding and Dosimetry (PSD) Program

Phy-X allows users to compute a wide range of material properties critical for assessing the shielding effectiveness of different substances. Among these parameters are the mass attenuation coefficient (μ/ρ), which describes the probability of gamma ray interaction per unit mass, and the linear attenuation coefficient (μ), which measures the attenuation per unit thickness of the material. The database also calculates the effective atomic number (Zeff), an important parameter for composite and multi-element materials, as well as the half-value layer (HVL) and tenth-value layer (TVL), which quantify the thickness of material required to reduce the gamma ray intensity to half and one-tenth of its original value, respectively. Additional parameters such as the electron density (Neff) and the mean free path (MFP), which provides the average distance traveled by photons within the material before interaction, are also available, offering a comprehensive insight into the material's interaction with radiation [7].

Phy-X is a versatile tool for analyzing photon interactions across a wide energy range, from 1 keV to 100 GeV. This broad spectrum makes it suitable for diverse applications, including medical imaging, nuclear power, industrial radiography, and aerospace research. Whether assessing low-energy X-rays for diagnostics or high-energy gamma rays for space exploration, Phy-X provides accurate tools to evaluate the shielding properties of materials. One of its key features is the ability to analyze custom materials by defining their elemental composition and density. This capability enables researchers to explore unconventional and eco-friendly alternatives to traditional shielding materials like lead, which, despite its effectiveness, poses environmental and health concerns [8]. Phy-X helps identify materials that combine high attenuation efficiency with desirable properties such as reduced weight, cost-effectiveness, and adaptability to specific needs. The platform integrates theoretical predictions with experimental data, ensuring accuracy and reliability in its outputs. Researchers can quickly screen and compare multiple materials, significantly reducing the time and effort needed for preliminary evaluations [9]. This is particularly valuable for industries with strict radiation safety standards, such as healthcare, nuclear energy, and aerospace [10]. Phy-X also supports innovation by optimizing shielding design while balancing performance, cost, and sustainability. Its user-friendly interface enables precise calculations, empowering researchers and engineers to develop efficient and sustainable shielding solutions tailored to industry-specific requirements. Accessible online at *https://phy-x.net/PSD*, Phy-X has become an essential tool for advancing radiation protection strategies. By combining precision, adaptability, and efficiency, it supports the development of effective shielding materials, contributing to improved safety and innovation in radiation-related industries. Whether for academic research or practical applications, Phy-X is a trusted platform for enhancing radiation safety and performance [4-6].

3 Results and Discussion

The molecular structure of glucose (C6H12O6) is depicted in **Figure 2**, showcasing both a three-dimensional ball-and-stick model and a two-dimensional structural formula. Glucose, a hexose monosaccharide, consists of six carbon (C) atoms, twelve hydrogen (H) atoms, and six oxygen (O) atoms, giving it a molar mass of 180.16 g/mol. The individual atoms contribute uniquely to the molecular weight: carbon has an atomic mass of about 12 atomic mass units (u), oxygen has an atomic mass of 16 u, and hydrogen has an atomic mass of 1 u. The precise atomic composition influences the chemical and physical properties of glucose, particularly its high water solubility.

The three-dimensional model emphasizes the spatial arrangement of glucose atoms, focusing on the pyranose ring structure formed by an intramolecular reaction between the aldehyde group at carbon-1 and the hydroxyl group at carbon-5. This reaction leads to the formation of a hemiacetal bond, resulting in a stable six-membered ring. The carbon atoms form the structural backbone, while oxygen atoms, present both in the ring and the hydroxyl (-OH) groups, are crucial in determining the molecule's polarity and reactivity. Hydrogen atoms fill the valence shells of carbon and oxygen, stabilizing the structure and enabling extensive hydrogen bonding. These hydroxyl groups make glucose highly hydrophilic, as they readily form hydrogen bonds with water molecules. This property enhances glucose's water solubility, allowing it to dissolve at approximately 91 grams per 100 milliliters of water at 25°C. This remarkable solubility is essential for glucose's role in biological systems. It allows glucose to function efficiently as the primary energy source for cellular respiration. Glucose is easily transported in the bloodstream, absorbed by cells, and utilized for energy production, making its molecular structure vital for energy metabolism and other physiological functions [11].

3.1 Linear attenuation coefficient (μL)

The relationship between the linear attenuation coefficient (μ) and thickness for the water-soluble organic compound C2H12O6 (glucose) was analyzed across various photon energies 133Ba (356) *keV*, 22Na (511 and 1275) *keV*, 137Cs (662) *keV*, and 60Co (1173 and 1333) *keV*. as depicted in **Figure 3**. To calculate the values of the linear attenuation coefficient for NCPs samples using the following the exponential equation (Lambert–Beer law) [12, 13].

$I=Ioe-\mu x$ (1)

eq. 1 can be written it as;

$\mu L=ln(I_oI)x/$ (2)

Where (x) is sample thickness, (μL) is linear attenuation coefficient, (Io) is unattenuated intensity of the monoenergetic photons narrow beam, (I) is attenuated intensity.

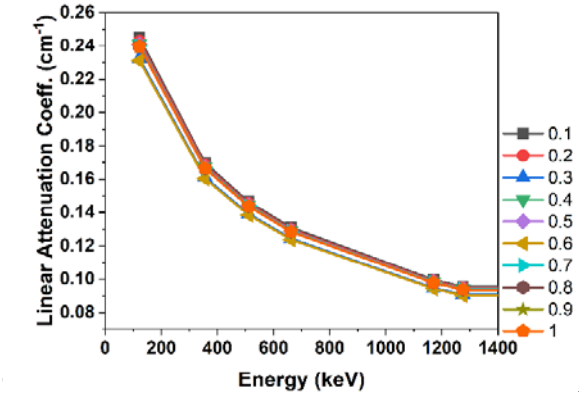

coefficient (cm^{-1}) for $C_2H_{12}O_6$ (Glucose) at different energy levels (keV) and concentrations. Overall, the linear attenuation coefficient decreases as the energy increases from 0 keV to 1400 keV, a trend consistent with the reduced interaction of higher-energy photons with matter. The different concentrations, represented by various markers and colors, exhibit a similar

decreasing pattern across the energy range. At lower energies (e.g., 50–100 keV), the attenuation coefficient shows a noticeable variation between concentrations, with higher concentrations displaying greater attenuation due to increased density. However, as the energy rises beyond 1000 keV, the curves converge, indicating that the dependence of attenuation on concentration diminishes at higher energies. This behavior aligns with the expectation that higher-energy photons are less affected by material density, resulting in less attenuation overall [14, 15].

3.2 Mass attenuation coefficient (μm)

Figure 2 illustrates the variation of the mass attenuation coefficient (μm) of the C2H12O6 as a function of photon energy across different thicknesses. The mass attenuation coefficient μm was obtained from the relation [16, 17];

$II_o = e^{-\mu\rho\rho x}$ (3)

eq. 3 can be written it as:

$\mu m = \mu\rho = ln(IoI)\rho x /$ (4)

Where, μρ is mass attenuation coefficient or μmwith unit cm2/g, ρ is a density of the sample with unit cm2/g and ρx is mass thickness. The graph depicts the mass attenuation coefficient (cm^2/g) 6

for $C_2H_{12}O_6$ (Glucose) across a range of photon energies (keV) for various concentrations. The mass attenuation coefficient decreases as photon energy increases, reflecting reduced photon interaction with the material at higher energies.

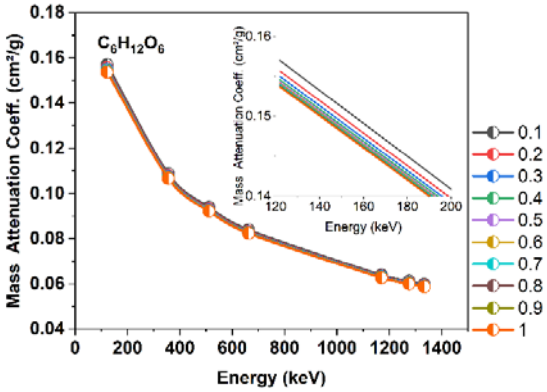

Figure 2 *Mass attenuation coefficient (μ/ρ) vs. Energy (keV) for C2H12O6*

All concentrations follow nearly identical curves, as the mass attenuation coefficient is normalized by density, making it largely independent of concentration. At lower photon energies (below 200 keV), the coefficient is higher due to dominant photoelectric effects, as highlighted in the inset graph. At higher photon energies (above 1000 keV), the curves converge, showing negligible variation among concentrations. This convergence aligns with the dominance of Compton scattering at higher energies, where the interaction depends less on the material's density. The graph effectively demonstrates the energy-dependent attenuation behavior of $C_2H_{12}O_6$ while confirming the minimal influence of concentration on mass attenuation coefficients [18].

3.3 HVL and TVL

The **Figure 3(a),(b)** illustrate the Half-Value Layer (HVL) and Tenth-Value Layer (TVL) for $C_2H_{12}O_6$ (Glucose) as functions of photon energy (keV) for various concentrations. Both HVL and TVL increase with photon energy, indicating that higher-energy photons penetrate deeper into the material before their intensity is reduced by half or to one-tenth, respectively. At lower photon energies, HVL and TVL values show a noticeable dependence on concentration, with higher concentrations resulting in smaller values due to increased attenuation efficiency. However, as photon energy increases (beyond ~1000 keV), the curves for different concentrations converge, reflecting reduced dependence on concentration as photon.

interactions become less density-sensitive. This behavior aligns with the dominance of photoelectric absorption at low energies and Compton scattering at high energies. The trends highlight the energy-dependent shielding properties of $C_2H_{12}O_6$ and the diminishing effect of concentration on attenuation at higher photon energies [19, 20].

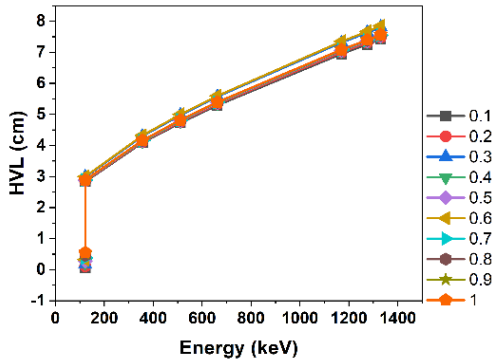

Figure 3(a) *Half-value layer (HVL) vs. Energy (keV) for C2H12O6*

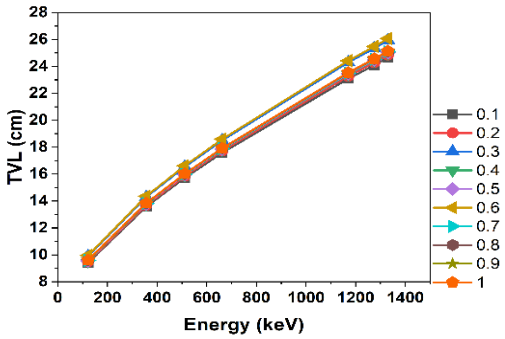

Figure 3(b) *Tenth-value layer (TVL) vs. Energy (keV) for C2H12O6*

3.4 σa and σe

The Figure 4(a),(b) represent the variation of effective atomic cross-section (σa) and effective electronic cross-section (σe) with energy (keV) for $C_2H_{12}O_6$. In the σa vs. energy graph, the σa values decrease gradually with increasing energy, showing a non-linear trend. At lower energy levels, σa values are higher, especially for lower concentrations, but these values converge as the energy increases. In the σe vs. energy graph, a similar trend is observed where σe decreases non-linearly with energy, showing a more pronounced decline at lower energy levels and stabilizing at higher energy values. The behavior remains consistent across varying concentrations, indicating a systematic dependence of cross-sections on energy and material composition. These trends are critical for understanding the attenuation and interaction properties of $C_2H_{12}O_6$ with different radiation energies [21, 22].

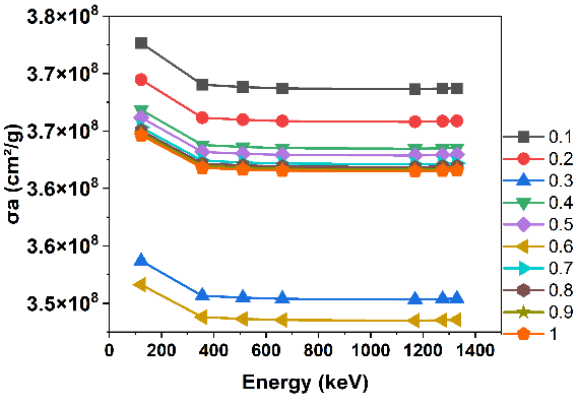

Figure 4(a) *Effective atomic cross-section (σa) vs. Energy (keV) for C2H12O6*

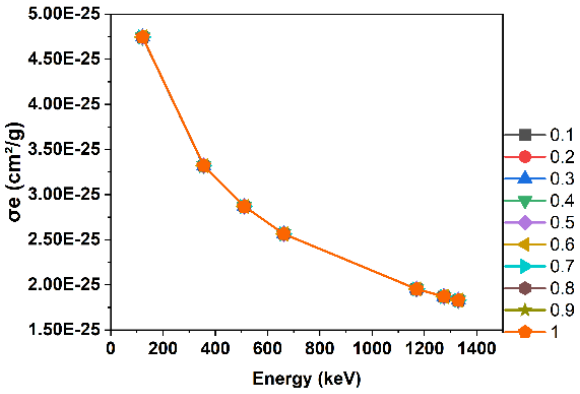

Figure 4(a) *Effective Electronic cross-section (σe) vs. Energy (keV) for C2H12O6*

1.3.5 Zeff

The Figure 5 depicts the variation of the effective atomic number (Zeff) with energy (keV) for $C_2H_{12}O_6$ at different concentrations. Zeff remains nearly constant across all concentrations at low to intermediate energy levels, up to approximately 1200 keV. This indicates stable photon interaction properties within this energy range, regardless of concentration changes [23].

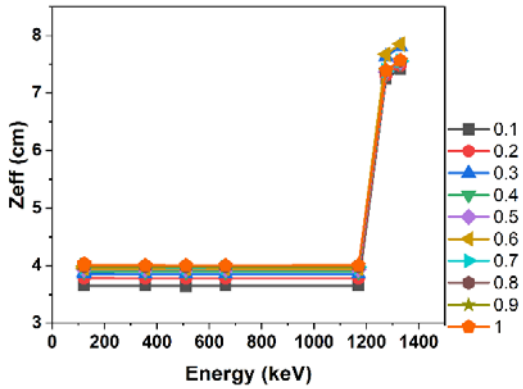

Figure 5 *effective atomic number (Zeff) with energy (keV) for C2H12O6*

A sharp increase in Zeff is observed beyond 1200 keV, likely due to the dominance of pair production interactions at higher photon energies, which are highly sensitive to atomic number. While the Zeff values are largely similar across concentrations, slight variations are noticeable during the high-energy transition, suggesting minor concentration effects in certain energy regions. These observations highlight the material's potential for applications in radiation shielding and dosimetry, where energy-dependent photon interactions play a critical role.

4 1.4 Conclusion

Theoretical measurements were carried out using narrow beam geometry and a NaI (Tl) detector, targeting gamma-ray energies from radioisotopes: 133Ba (356) keV, 22Na (511 and 1275) keV, 137Cs (662) keV, and 60Co (1173 and 1333) keV using Phy-X database. In conclusion, shielding against cosmic gamma rays is a critical aspect of space exploration, requiring materials that balance high attenuation efficiency with practical considerations such as weight, adaptability, and environmental impact. Traditional shielding materials like lead,

while effective, pose health and environmental challenges, prompting the search for alternative solutions. Water-soluble organic compounds like glucose ($C_6H_{12}O_6$) emerge as promising candidates due to their cost-effectiveness, reduced density, and flexibility. Advancements in radiation protection technologies and computational tools, such as Phy-X, have greatly facilitated the evaluation and optimization of shielding materials. Phy-X offers precise calculations of critical parameters, including the mass attenuation coefficient (μ/ρ), linear attenuation coefficient (μ), effective atomic number (Zeff), and other essential properties like HVL, TVL, Neff, and MFP. This platform provides a reliable resource for analyzing and comparing materials, thereby expediting innovation in radiation shielding design. Analysis of glucose's shielding properties reveals energy-dependent trends in attenuation and interaction parameters. The linear attenuation coefficient and cross-sections decrease with increasing photon

energy, with photoelectric absorption dominating at lower energies and Compton scattering taking precedence at higher energies. The effective atomic number (Zeff) exhibits a sharp increase at energies beyond 1200 keV, corresponding to the onset of pair production, underscoring glucose's potential in high-energy radiation shielding applications. Phy-X supports the exploration of unconventional materials like glucose, enabling researchers to develop efficient, sustainable, and application-specific shielding solutions. By advancing the understanding of radiation-material interactions, these efforts contribute significantly to safer and more innovative approaches in radiation protection for space exploration and beyond.

5 Reference

[1] S.-C. Kim, Analysis of shielding performance of radiation-shielding materials according to particle size and clustering effects, Applied Sciences, 11 (2021) 4010.

[2] N.J. AbuAlRoos, M.N. Azman, N.A.B. Amin, R. Zainon, Tungsten-based material as promising new lead-free gamma radiation shielding material in nuclear medicine, Physica Medica, 78 (2020) 48-57.

[3] S. Prabhu, S. Bubbly, S.B. Gudennavar, X-ray and γ-ray shielding efficiency of polymer composites: choice of fillers, effect of loading and filler size, photon energy and multifunctionality, Polymer Reviews, 63 (2023) 246-288.

[4] M. Hasan, S. Sugiharto, S. Astutiningsih, Gamma radiation shielding properties of slag and fly ash-based geopolymers, Atom Indonesia, 47 (2021) 173-180.

[5] A.I. Osman, S. Fawzy, M. Farghali, M. El-Azazy, A.M. Elgarahy, R.A. Fahim, M.A. Maksoud, A.A. Ajlan, M. Yousry, Y. Saleem, Biochar for agronomy, animal farming, anaerobic digestion, composting, water treatment, soil remediation, construction, energy storage, and carbon sequestration: a review, Environmental Chemistry Letters, 20 (2022) 2385-2485. 10

[6] Y. Zhao, L. Hao, X. Zhang, S. Tan, H. Li, J. Zheng, G. Ji, A novel strategy in electromagnetic wave absorbing and shielding materials design: multi-responsive field effect, Small Science, 2 (2022) 2100077.

[7] E. Şakar, Ö.F. Özpolat, B. Alım, M. Sayyed, M. Kurudirek, Phy-X/PSD: development of a user friendly online software for calculation of parameters relevant to radiation shielding and dosimetry, Radiation Physics and Chemistry, 166 (2020) 108496.

[8] A. Aşkın, Evaluation of the radiation shielding capabilities of the Na2B4O7–SiO2–MoO3-Dy2O3 glass quaternary using Geant4 simulation code and Phy-X/PSD database, Ceramics International, 46 (2020) 9096-9102.

[9] M. Alhassan, J. Baraya, A. Garba, Accuracy of Phy-X/PSD Software Compared to XCOM in the Determination of Mass Attenuation Coefficient of Glass Systems, Journal of Applied Sciences and Environmental Management, 27 (2023) 985-988.

[10] K. Gunoglu, H.V. Özkavak, İ. Akkurt, Evaluation of gamma ray attenuation properties of boron carbide (B4C) doped AISI 316 stainless steel: Experimental, XCOM and Phy-X/PSD database software, Materials Today Communications, 29 (2021) 102793.

[11] A.T. Naikwadi, B.K. Sharma, K.D. Bhatt, P.A. Mahanwar, Gamma radiation processed polymeric materials for high performance applications: a review, Frontiers in Chemistry, 10 (2022) 837111.

[12] V. Mosorov, The Lambert-Beer law in time domain form and its application, Applied Radiation and Isotopes, 128 (2017) 1-5.

[13] S. Dongarge, S. Mitkar, Measurement of linear and mass attenuation coefficient of alcohol soluable compound for gamma-rays at energy 0.36 MeV, Journal of Chemical and Pharmaceutical Research, 4 (2012) 3116-3120.

[14] T.A.A. Junior, M.S. Nogueira, V. Vivolo, M. Potiens, L. Campos, Mass attenuation coefficients of X-rays in different barite concrete used in radiation protection as shielding against ionizing radiation, Radiation Physics and Chemistry, 140 (2017) 349-354.

[15] Gagandeep, K. Singh, B. Lark, H. Sahota, Attenuation measurements in solutions of some carbohydrates, Nuclear science and engineering, 134 (2000) 208-217.

[16] C.V. More, H. Alavian, P.P. Pawar, Evaluation of gamma-ray attenuation characteristics of some thermoplastic polymers: Experimental, WinXCom and MCNPX studies, Journal of Non-Crystalline Solids, 546 (2020) 120277.

[17] S. Mitkar, S. Dongarge, Study the Linear and Mass Attenuation Coefficient of Alcohol Soluble Compound for Gamma Rays at Energy 662 KeV, J. Chem. Pharm. Res, 4 (2012) 3944-3949.

[18] N. Ramachandran, K.K. Nair, K. Abdullah, K. Varier, Photon interaction studies using 241 Am γ-rays, Pramana, 67 (2006) 507-517.

[19] P.S. Dahinde, G. Dapke, S. Raut, R. Bhosale, P.P. Pawar, Analysis of half value layer (HVL), tenth value layer (TVL) and mean free path (MFP) of some oxides in the energy range of 122KeV to 1330KeV, Indian Journal of Scientific Research, 9 (2019) 79-84. 11

[20] N. Nagaraja, H.C. Manjunatha, K.N. Sridhar, N. Sowmya, L. Seenappa, R. Munirathnam, R. Soundar, An innovative approach for estimating energy absorption buildup factors (EABF) with HVL and TVL, Radiation protection dosimetry, 199 (2023) 2447-2454.

[21] N. Alallak, S. Sarhan, Factors affecting gamma ray transmission, DOI (2012).

[22] D.K. Gaikwad, P.P. Pawar, T.P. Selvam, Mass attenuation coefficients and effective atomic numbers of biological compounds for gamma ray interactions, Radiation Physics and Chemistry, 138 (2017) 75-80.

[23] M. Tahmasebi Birgani, F. Seif, N. Chegeni, M. Bayatiani, Determination of the effective atomic and mass numbers for mixture and compound materials in high energy photon interactions, Journal of Radioanalytical and Nuclear Chemistry, 292 (2012) 1367-1370.